

# Theoretical Isotropic Dissolution of Nonspherical Particles

PETER VENG PEDERSEN \* and K. F. BROWN

**Abstract** □ Equations are derived for the isotropic dissolution of single particles, considering simple forms of the six crystal systems. These can be summarized by three basic equations which are approximated well, and in some cases exactly, by the dissolution equation for a hypothetical spherical particle of specified diameter. Formulas are given to enable calculation of this diameter and to minimize the weighted errors in the approximations. Spherical approximations provide a simple basis for calculating the dissolution profile of real multiparticulate systems which are difficult to describe otherwise. Spherical approximations based on equal surface area or volume result in large errors.

**Keyphrases** □ Dissolution, isotropic—nonspherical particles, six crystal systems, equations derived □ Isotropic dissolution—nonspherical particles, six crystal systems, equations derived □ Particles, nonspherical— isotropic dissolution, six crystal systems, equations derived □ Crystal systems, various—nonspherical particles, isotropic dissolution, equations derived

The influence of shape factors on dissolution kinetics of drugs has been discussed for tablets and time-released tablets (1, 2), but little attention has been given to single drug particles (3, 4). Most dissolution kinetic models consider spherical particles. Application of such models to real particle systems is complicated by the fact that pure drug particles are not spherical. The usual approach has been to treat the real particles as hypothetical spherical particles having the same surface area or volume. Such approximations may introduce substantial errors.

This paper presents exact isotropic single-particle dissolution equations for several nonspherical forms and formulas, enabling calculation of the diameters of hypothetical spherical particles which closely approximate the dissolution of these forms.

## THEORY

Assume that dissolution takes place isotropically, that is, that the rate of dissolution per unit surface area,  $J$ , is constant so that the following equation can be written:

$$\frac{dw}{dt} = -JA \quad (\text{Eq. 1})$$

where  $w$  is the amount undissolved, and  $A$  is the surface area. This equation implies that the boundary of a plane interface retreats with constant speed during dissolution such that:

$$\frac{ds}{dt} = -\frac{J}{\rho} \quad (\text{Eq. 2})$$

where  $\rho$  is the density, and  $s$  is the distance perpendicular to the interface from some fixed reference point in the dissolving solid. Equation 2 integrates to:

$$s = s_0 - \frac{J}{\rho} t \quad (\text{Eq. 3})$$

where  $s_0$  is the initial ( $t = 0$ ) distance to the reference point. When this equation is applied to the isotropic dissolution of a spherical

particle, the following equation arises:

$$\frac{w}{w_0} = \left(1 - \frac{J}{r_0\rho} t\right)^3 \quad (\text{Eq. 4})$$

or:

$$\left(\frac{w}{w_0}\right)^{1/3} = 1 - \frac{J}{r_0\rho} t \quad (\text{Eq. 5})$$

where  $r_0$  is the initial radius of the particle.

Therefore, when a spherical particle dissolves isotropically ( $J = \text{constant}$ ), it obeys the Hixson and Crowell (5) cube root law; that is, a plot of  $(w/w_0)^{1/3}$  versus time is linear.

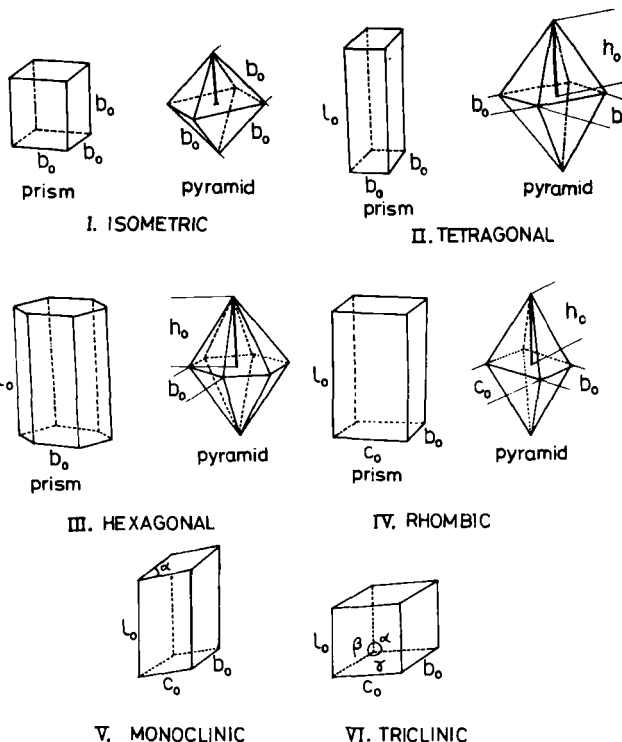
**Dissolution of Prismatic Particles**—Structures I–VI are 10 simple forms of the six crystal systems and illustrate the dimensional quantities  $b_0$ ,  $c_0$ ,  $l_0$ ,  $h_0$ , and  $\alpha$  used in the following derivations. It is assumed that  $b_0 < c_0 < l_0$ .

Consider a prismatic particle of initial length  $l_0$  and having a regular  $n$ -gonal cross section with side of initial length  $b_0$ . The distance,  $s$ , from the  $n$  sides of the polygon to the center as reference point decreases during dissolution according to Eq. 3. The area of the cross section at any time is then equal to  $n[s_0 - (J/\rho)t]^2 \tan(\pi/n)$ , and the length of the prism is equal to  $l_0 - (2J/\rho)t$ , so the particle weight at time  $t$  is:

$$w = \rho \left(l_0 - \frac{2J}{\rho} t\right) n \left(s_0 - \frac{J}{\rho} t\right)^2 \tan \frac{\pi}{n} \quad (\text{Eq. 6})$$

which, since  $s_0 = (b_0/2) \cot(\pi/n)$ , can be written as:

$$w = \rho \left(l_0 - \frac{2J}{\rho} t\right) \frac{n}{4} \left[b_0 - \left(\frac{2J}{\rho} \tan \frac{\pi}{n}\right) t\right]^2 \quad (\text{Eq. 7})$$



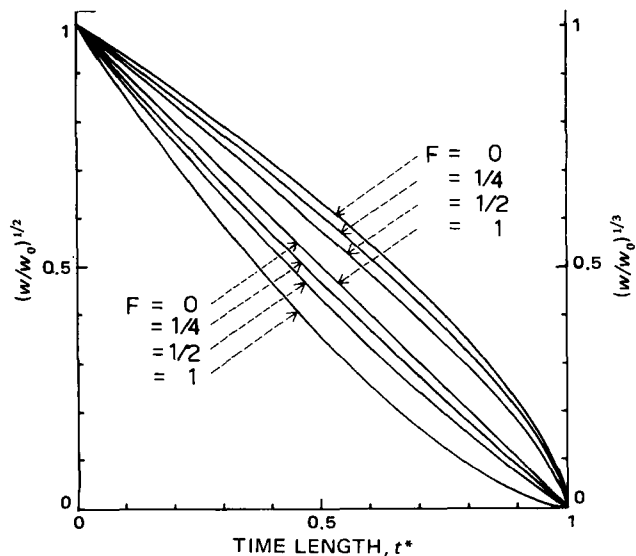


**Figure 1**—Influence of the shape ratio,  $F$ , on the intrinsic dissolution profile of an  $n$ -gonal prismatic particle (tetragonal or hexagonal) or a rhombic pyramidal particle. The four curves below and including the diagonal are square root plots. The four curves above and including the diagonal are cube root plots. The dissolution deviates increasingly from the  $(w/w_0)^{1/3}$  versus  $t^*$  linear relationship (the cube root law) as the shape ratio becomes less than 1 and approaches a linear  $(w/w_0)^{1/2}$  versus  $t^*$  relationship (the square root law).

At  $t = 0$ ,  $w_0 = \rho l_0(n/4)b_0^2$ , so Eq. 7 can be written:

$$\frac{w}{w_0} = \left(1 - \frac{2J}{l_0\rho}t\right) \left[1 - \left(\frac{2J}{b_0\rho} \tan \frac{\pi}{n}\right)t\right]^2 \quad (\text{Eq. 8})$$

Equation 8 comprises the exact dissolution equations for the prismatic forms of the isometric ( $n = 4$ ,  $b_0 = l_0$ ), tetragonal ( $n = 4$ ,  $b_0 = l_0$ ), and hexagonal ( $n = 6$ ) crystal systems (I–III). The rhombic prism, having a rectangular cross section, dissolves according to:

$$w = \rho \left(b_0 - \frac{2J}{\rho}t\right) \left(c_0 - \frac{2J}{\rho}t\right) \left(l_0 - \frac{2J}{\rho}t\right) \quad (\text{Eq. 9})$$

because of the isotropic retreat of all surfaces. Similarly to Eq. 8, this equation can be written:

$$\frac{w}{w_0} = \left(1 - \frac{2J}{b_0\rho}t\right) \left(1 - \frac{2J}{c_0\rho}t\right) \left(1 - \frac{2J}{l_0\rho}t\right) \quad (\text{Eq. 10})$$

The monoclinic prismatic particle, having a parallelogram cross section with an acute angle  $\alpha$ , has at any time a cross-sectional area equal to  $bc \sin \alpha$ , where  $b = b_0 - [(2J/\rho) \sin \alpha]t$  and  $c = c_0 - [(2J/\rho) \sin \alpha]t$ , so it dissolves according to:

$$w = \rho \left(l_0 - \frac{2J}{\rho}t\right) \left[b_0 - \left(\frac{2J}{\rho} \sin \alpha\right)t\right] \times \left[c_0 - \left(\frac{2J}{\rho} \sin \alpha\right)t\right] \sin \alpha \quad (\text{Eq. 11})$$

or:

$$\frac{w}{w_0} = \left(1 - \frac{2J}{l_0\rho}t\right) \left[1 - \left(\frac{2J}{b_0\rho} \sin \alpha\right)t\right] \times \left[1 - \left(\frac{2J}{c_0\rho} \sin \alpha\right)t\right] \quad (\text{Eq. 12})$$

**Dissolution of Pyramidal Particles**—The regular pyramidal forms of the isometric, tetragonal, and hexagonal systems (I–III) all dissolve like a spherical particle, following the “cube root law”: all plane surfaces of the pyramid retreat toward its center of symmetry with the same constant speed during isotropic dissolution. Therefore, the shape of the pyramid remains the same while its size diminishes. It can, for example, be shown geometrically that all lengths of the prism decrease by a factor of  $1 - (J/r_0\rho)t$ , where  $r_0$ , given by:

$$r_0 = \frac{h_0 b_0}{2\sqrt{h_0^2 + b_0^2/4}} \quad (\text{Eq. 13})$$

is the radius of the largest sphere that can be contained in the pyramid initially. The weight of the regular  $n$ -gonal prism at time  $t$  is equal

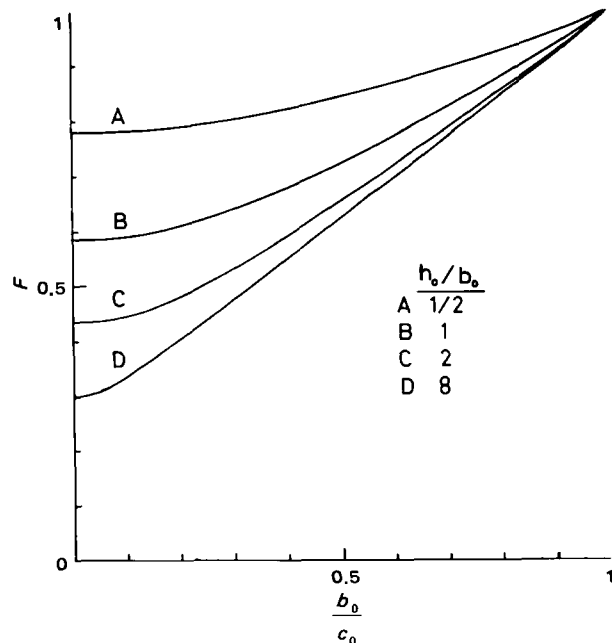


**Figure 2**—Variation of the shape ratio,  $F$ , of a rhombic pyramidal particle having various shapes (see Structure IV for definitions of  $b_0$ ,  $c_0$ , and  $h_0$ ).

to  $\frac{1}{6}\rho n h_t b_t^2 \cot(\pi/n)$ , where the height,  $h_t$ , and side,  $b_t$ , are  $h_t = h_0[1 - (J/r_0\rho)t]$  and  $b_t = b_0[1 - (J/r_0\rho)t]$ , respectively, according to the above theory. Thus, its weight is:

$$w = \frac{1}{6}\rho n h_0 b_0^2 \left(1 - \frac{J}{r_0\rho}t\right)^3 \cot \frac{\pi}{n} \quad (\text{Eq. 14})$$

from which it follows that:

$$\frac{w}{w_0} = \left(1 - \frac{J}{r_0\rho}t\right)^3 \quad (\text{Eq. 15})$$

This equation is identical to Eq. 4. Therefore, a regular pyramidal crystal form dissolves in exactly the same way as the largest (hypothetical) spherical particle that can be contained within its boundaries initially. This is also approximately true for an irregular pyramidal form such as the rhombic pyramid when the irregularity is not too extreme. It can be shown, using a double integration approach, that this crystal form dissolves according to:

$$\frac{w}{w_0} = \left(1 - \frac{J}{r_1\rho}t\right)^2 \left[1 - \left(\frac{1}{4r_1} + \frac{3}{4r_2}\right)\frac{J}{\rho}t\right] \quad (\text{Eq. 16})$$

where:

$$r_1 = \frac{h_0 b_0}{2\sqrt{h_0^2 + b_0^2/4}} \quad (\text{Eq. 17})$$

$$r_2 = \frac{h_0 c_0}{2\sqrt{h_0^2 + c_0^2/4}} \quad (\text{Eq. 18})$$

The deviation from spherical particle dissolution (Eq. 15) arises from the fact that  $b_0 < c_0$ . If  $b_0 = c_0$ , then Eq. 16 reduces to the special case of Eq. 15 as expected.

To evaluate these single-particle dissolution equations, it is convenient to present them in a transformed simplified form which better illustrates their *intrinsic dissolution profile*<sup>1</sup>. For example, Eq. 8 can be transformed to:

$$\frac{w}{w_0} = (1 - Ft^*)(1 - t^*)^2 \quad (\text{Eq. 19})$$

or:

$$\left(\frac{w}{w_0}\right)^{1/3} = (1 - Ft^*)^{1/3}(1 - t^*)^{2/3} \quad (\text{Eq. 20})$$

<sup>1</sup> The concept of “intrinsic dissolution profile” was defined and discussed previously (6). It provides a powerful basis for the analysis of multiparticle dissolution kinetics. In the case of single-particle dissolution, it enables the evaluation of the *shape* of the dissolution curve irrespective of the way time is scaled.

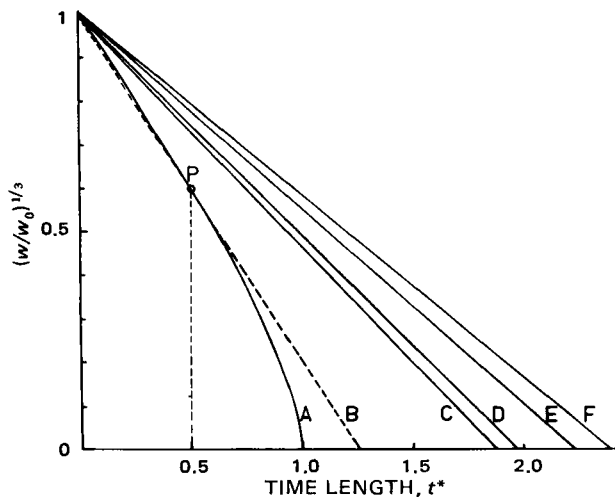


**Figure 3**—Application of the use of spherical approximations to describe the dissolution of an  $n$ -gonal prismatic particle (curve A, Eq. 20,  $F = 1/4$ ). Curves C and E represent the dissolution of a spherical particle with the same volume (Eq. 27,  $F = 1/4$ ,  $n = 4, 6$ ). Similarly, curves D and F represent a spherical particle having the same surface area (Eq. 26,  $F = 1/4$ ,  $n = 4, 6$ ). Curve B is the approximation (Eq. 30,  $F = 1/4$ ) from which the equivalent spherical diameter is calculated (Eq. 31).

where:

$$t^* = \left( \frac{2J}{b_0\rho} \tan \frac{\pi}{n} \right) t \quad (\text{Eq. 21})$$

is denoted time length and:

$$F = \frac{b_0}{l_0} \cot \frac{\pi}{n} \quad (\text{Eq. 22})$$

is denoted the shape ratio. This form of the equation clearly shows that the intrinsic dissolution profile depends only on the value of the dimensionless shape ratio,  $F$ , which defines the particle shape. Furthermore, the transformation makes it more convenient to evaluate the extent to which dissolution of the prismatic particle deviates from spherical particle dissolution (*i.e.*, from the cube root law). For  $F = 1$ , *i.e.*, when  $(w/w_0)^{1/3} = 1 - t^*$ , there is no such deviation; however, as  $F$  decreases, the deviation becomes more significant, *i.e.*, when the length of the particle relative to its side length or "diameter" becomes more extreme.

It is seen (Fig. 1) that as  $F$  decreases, the deviation from the cube root law becomes larger. Dissolution then approaches what can be called "the square root law," that is, a linear relationship between  $(w/w_0)^{1/2}$  and time length (or time). This is in agreement with the fact that, for small  $F$  values, Eq. 19 approximates  $(w/w_0)^{1/2} = 1 - t^*$ . The cube root law and the square root law were each postulated previously as a model for the dissolution of a spherical particle under sink conditions (5, 7). Pure drug particles are not spherical, however, but are often prismatic in shape. Therefore, the particle shape effect should be considered in any experimental evaluation of such models.

The dissolution equation for a rhombic pyramidal particle (Eq. 16) can also be transformed to Eq. 19 where:

$$t^* = \left( \frac{2J}{\rho} \sqrt{h_0^2 + b_0^2/4} \right) t \quad (\text{Eq. 23})$$

and:

$$F = \frac{1}{4} + \frac{3}{4} \sqrt{\frac{h_0^2 + c_0^2/4}{h_0^2 + b_0^2/4}} \quad (\text{Eq. 24})$$

It is seen (Fig. 2) that the shape ratio,  $F$ , for this pyramidal particle form does not deviate much from 1 for most shapes, indicating that in most cases dissolution closely approximates that of a spherical particle.

Dissolution equations for either a rhombic (Eq. 10) or a monoclinic (Eq. 12) particle can be written similarly, in a common transformed form, as:

$$\frac{w}{w_0} = (1 - F_1 t^*)(1 - F_2 t^*)(1 - t^*) \quad (\text{Eq. 25})$$

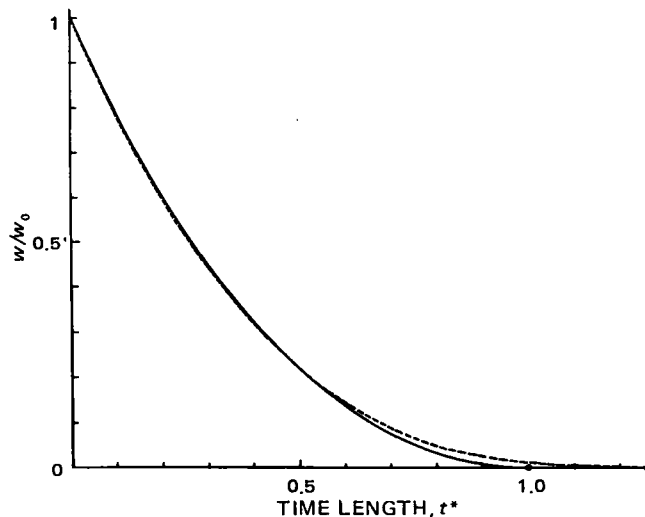


**Figure 4**—Dissolution of an  $n$ -gonal prismatic particle (tetragonal or hexagonal) or a rhombic pyramidal particle having the shape ratio  $F = 1/4$  (unbroken line, Eq. 19) and a hypothetical spherical particle (broken line) representing the approximation (Eq. 30) from which the equivalent spherical diameter is calculated (Eq. 31).

where  $F_1 = (b_0/c_0)$ ,  $F_2 = (b_0/l_0)$ , and  $t^* = (2J/b_0\rho)t$  for a rhombic particle and  $F_1 = (b_0/c_0)$ ,  $F_2 = (b_0/l_0) \sin \alpha$ , and  $t^* = (2J/b_0\rho \sin \alpha)t$  for a monoclinic particle.

## RESULTS AND DISCUSSION

The main objective of studying single-particle dissolution kinetics is to gain a better understanding and description of multiparticulate systems. In practice, the particles in such a system vary both in size and shape, thus making a rigorous mathematical description quite complex. Such a description must include a bivariate distribution function of the particle dimensions, and evaluation of this distribution function is rather difficult.

A considerable simplification can be achieved, however, if the dissolution of each particle in the multiparticulate sphere can be approximated by the dissolution of a hypothetical spherical particle of some specified diameter. The problem associated with the bivariate distribution function is then avoided, since the system is simplified to contain only one dimensional variable, the diameter of the spheres. The exact dissolution profile of the hypothetical particle system that approximates the real system can then be calculated using an equation presented previously (6, 8).

The usual approach to describe dissolution of nonspherical particles has been to approximate them by spherical particles having the same surface area or volume. It is of interest to evaluate the errors in such approximations. A spherical particle, having the same surface area as an  $n$ -gonal prismatic particle with shape ratio  $F$ , dissolves according to:

$$\left( \frac{w}{w_0} \right)^{1/3} = 1 - \sqrt{\frac{2\pi \cot \frac{\pi}{n}}{n(1+2/F)}} t^* \quad (\text{Eq. 26})$$

Or, if it has the same volume, it dissolves according to:

$$\left( \frac{w}{w_0} \right)^{1/3} = 1 - \left( \frac{2\pi F \cot \frac{\pi}{n}}{3n} \right)^{1/3} t^* \quad (\text{Eq. 27})$$

where  $t^*$  and  $F$  are defined by Eqs. 21 and 22. Figure 3 shows the substantial errors introduced by such approximations based on equal surface area or volume. This is not only the case for  $F = 1/4$  but for all other values of the shape ratio less than 1.

The problem of finding the diameter of the spherical particle that best approximates the dissolution of an  $n$ -gonal prismatic particle is mathematically the same as finding a quantity,  $x$ , such that:

$$\frac{w}{w_0} = (1 - xt^*)^3 \quad (\text{Eq. 28})$$

best fits Eq. 19. Possibly the best criterion for this fit is to minimize

**Table I—Summary of the Dissolution of the Particle Forms Including Expressions for Calculating the Equivalent Spherical Diameter**

Dissolution of Prismatic Particles <sup>a</sup>				
<u><i>n</i>-Gonal Prismatic Particles</u>				
	Exact dissolution equation	$\frac{w}{w_0} = (1 - Ft^*)(1 - t^*)^2$		
	Spherical approximation	$\frac{w}{w_0} \doteq \{1 - [2 - (2 - F)^{1/3}]t^*\}^3$		
Crystal System	Time Length, <i>t</i> *	Shape Ratio <sup>b</sup> , <i>F</i>	Equivalent Spherical Diameter $a = \frac{2Jt}{[2 - (2 - F)^{1/3}]\rho t^*}$	
<i>n</i> -Gonal	$\left(\frac{2J}{b_0\rho} \tan \frac{\pi}{n}\right)t$	$\frac{b_0}{l_0} \cot \frac{\pi}{n}$	$\frac{b_0 \cot \frac{\pi}{n}}{2 - \left(2 - \frac{b_0}{l_0} \cot \frac{\pi}{n}\right)^{1/3}}$	
Tetragonal ( <i>n</i> = 4)	$\frac{2J}{b_0\rho} t$	$\frac{b_0}{l_0}$	$\frac{b_0}{2 - \left(2 - \frac{b_0}{l_0}\right)^{1/3}}$	
Isometric ( <i>n</i> = 4, <i>b</i> <sub>0</sub> = <i>l</i> <sub>0</sub> )	$\frac{2J}{b_0\rho} t$	1	<i>b</i> <sub>0</sub>	
Hexagonal ( <i>n</i> = 6)	$\frac{2\sqrt{3}J}{3b_0\rho} t$	$\sqrt{3} \frac{b_0}{l_0}$	$\frac{\sqrt{3}b_0}{2 - \left(2 - 3 \frac{b_0}{l_0}\right)^{1/3}}$	
<u>Rhombic and Monoclinic Particles</u>				
	Exact dissolution equations	$\frac{w}{w_0} = (1 - F_1t^*)(1 - F_2t^*)(1 - t^*)$		
	Spherical approximation	$\frac{w}{w_0} \doteq \{1 - [2 - (2 - F_1)^{1/3}(2 - F_2)^{1/3}]t^*\}^3$		
Crystal System	Time Length, <i>t</i> *	Shape Ratios		Equivalent Spherical Diameter $a = \frac{2Jt}{[2 - (2 - F_1)^{1/3}(2 - F_2)^{1/3}]\rho t^*}$
		<i>F</i> <sub>1</sub>	<i>F</i> <sub>2</sub>	
Rhombic	$\frac{2J}{b_0\rho} t$	$\frac{b_0}{c_0}$	$\frac{b_0}{l_0}$	$\frac{b_0}{2 - \left(2 - \frac{b_0}{c_0}\right)^{1/3} \left(2 - \frac{b_0}{l_0}\right)^{1/3}}$
Monoclinic	$\frac{2J}{b_0\rho \sin \alpha} t$	$\frac{b_0}{c_0}$	$\frac{b_0}{l_0} \sin \alpha$	$\frac{b_0 \sin \alpha}{2 - \left(2 - \frac{b_0}{c_0}\right)^{1/3} \left(2 - \frac{b_0}{l_0} \sin \alpha\right)^{1/3}}$
Dissolution of Pyramidal Particles				
<u><i>n</i>-Gonal Pyramidal Particles (Isometric, Tetragonal, Hexagonal)</u>				
	Exact dissolution equation	$\frac{w}{w_0} = (1 - t^*)^3$		
	Time length	$t^* = \frac{2J\sqrt{h_0^2 + b_0^2/4}}{\rho} t$		
	Equivalent spherical diameter <sup>c</sup>	$a = \frac{h_0 b_0}{\sqrt{h_0^2 + b_0^2/4}}$		
<u>Rhombic Pyramidal Particles</u>				
	Exact dissolution equation	$\frac{w}{w_0} = (1 - Ft^*)(1 - t^*)^2$		

Table I—(Continued)

Spherical approximation	$\frac{w}{w_0} \doteq \{1 - [2 - (2 - F)^{1/3}] t^*\}^3$
Time length	$t^* = \frac{2J\sqrt{h_0^2 + b_0^2/4}}{\rho} t$
Shape ratio	$F = \frac{1}{4} + \frac{3}{4} \sqrt{\frac{h_0^2 + c_0^2/4}{h_0^2 + b_0^2/4}}$
Equivalent spherical diameter	$a = \frac{1}{[2 - (2 - F)^{1/3}] \sqrt{h_0^2 + b_0^2/4}}$

<sup>a</sup>Structures I–VI illustrate the quantities  $b_0$ ,  $c_0$ ,  $l_0$ , and  $\alpha$  used. <sup>b</sup>When  $F = 1$ , i.e.,  $(b_0/l_0) = \tan(\pi/n)$ , then the equivalent spherical diameter is equal to the biggest sphere that can be contained in the prismatic body. The spherical approximation of the dissolution then becomes exact. <sup>c</sup>This diameter is equal to the biggest sphere the pyramid can contain.

the sum of the squared errors where these are weighted proportionally to  $w/w_0$ , i.e., to minimize the integral:

$$I = \int_0^1 [(1 - Ft^*)(1 - t^*)^2 - (1 - xt^*)^3]^2 \times (1 - Ft^*)(1 - t^*)^2 dt^* \quad (\text{Eq. 29})$$

by solving for  $x$  when  $\partial I/\partial x = 0$ . The exact expression for  $x$  is too complex to be of value. However, a very good approximation was obtained by choosing  $x$  such that Eqs. 28 and 19 intersect at  $t^* = 1/2$  (point P, Fig. 3), which corresponds to  $x = 2 - (2 - F)^{1/3}$ , such that the dissolution is approximated by the following equation for the hypothetical spherical particle:

$$\left(\frac{w}{w_0}\right)^{1/3} = 1 - [2 - (2 - F)^{1/3}]t^* \quad (\text{Eq. 30})$$

The equivalent spherical diameter,  $a$ , i.e., the diameter of this spherical particle, can then be obtained by equating the right-hand sides of Eqs. 30 and 5 from which it follows that:

$$a = \frac{2Jt}{[2 - (2 - F)^{1/3}] \rho t^*} \quad (\text{Eq. 31})$$

Although the approximation given by Eq. 30 (curve B, Fig. 3) does not seem to be a particularly good fit to the exact dissolution curve calculated for the  $n$ -gonal particle (curve A), when the same two curves are plotted as  $w/w_0$  versus time length (Fig. 4) instead of as  $(w/w_0)^{1/3}$ , it is clear that this is because of the nonlinear scaling in the cube root plot. The stippled curve (Fig. 4) representing the spherical approximation shows excellent fit to the true dissolution. The weighted errors of the spherical approximation were calculated for various values of the shape ratio  $F$  and showed (Fig. 5) that this choice for the approximation was satisfactory.

By using similar reasoning, it was found that the equation:

$$\left(\frac{w}{w_0}\right)^{1/3} = 1 - [2 - (2 - F_1)^{1/3}(2 - F_2)^{1/3}]t^* \quad (\text{Eq. 32})$$

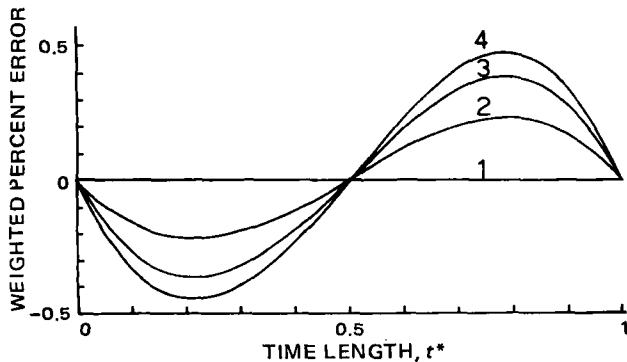


Figure 5—Graph of errors in the spherical approximation (Eq. 30) of the dissolution (Eq. 19) of an  $n$ -gonal prismatic particle (isometric, tetragonal, or hexagonal) or a rhombic pyramidal particle of different shape ratios. The error is weighted proportionally to the fraction undissolved ( $w/w_0$ ). Key: 1,  $F = 1$ ; 2,  $F = 1/2$ ; 3,  $F = 1/3$ ; and 4,  $F = 1/4$ .

which is similar in form to Eq. 30, provides a good spherical approximation to Eq. 25, which describes the dissolution of rhombic and monoclinic prismatic particles. The equivalent spherical diameter in these cases is given by:

$$a = \frac{2Jt}{[2 - (2 - F_1)^{1/3}(2 - F_2)^{1/3}] \rho t^*} \quad (\text{Eq. 33})$$

The error in this spherical approximation (Eq. 32) is substantially greater in the final stages of the dissolution process (Figs. 6 and 7) than in the previous case (Figs. 4 and 5). However, a previous study (8) showed that dissolution of a nonuniformly distributed, multiparticulate system is only slightly affected by the dissolution behavior of the smallest particles. Substantial truncation at the lower end of the particle-size distribution had very little effect on the dissolution profile calculated (8). Thus, approximation error in the later stage of the single-particle dissolution does not introduce the same degree of error when applied to a nonuniformly distributed, multiparticulate system. The approximation (Eq. 32) should, therefore, yield considerably better results when applied to a multiparticulate system than might be judged from Fig. 6. This explains the choice of the particular weighting of the errors in the approximation procedure.

Table I summarizes the dissolution of the particle forms shown in Structures I–VI and gives formulas for the calculation of the equivalent spherical diameter in each case<sup>2</sup>. The dissolution of these 10 forms can be described by three basic transformed equations of cubic form in time length (or time). The dissolution can thus be described exactly by a third degree polynomial in time in all cases.

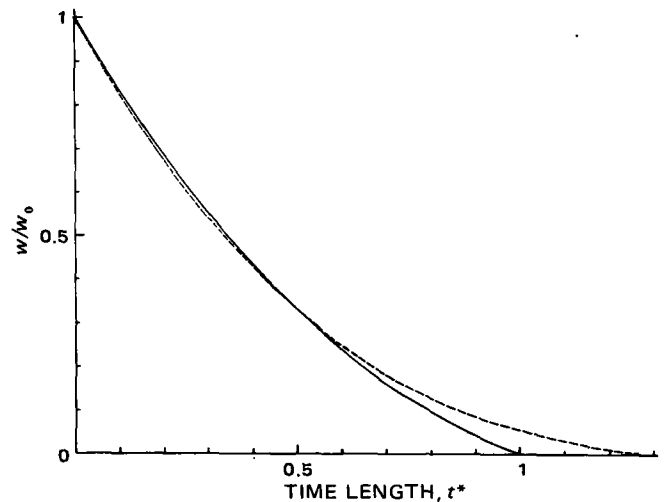
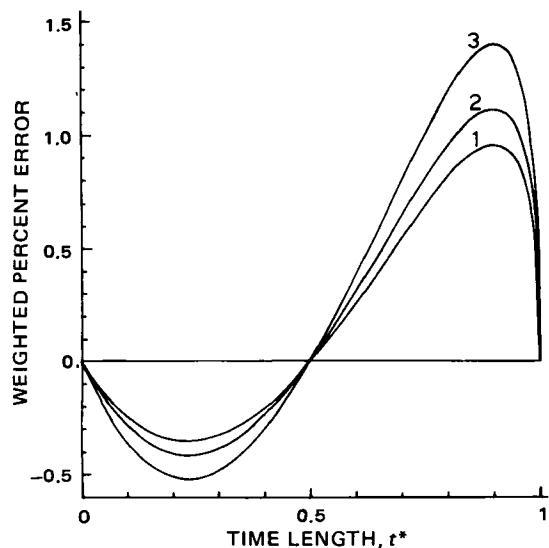


Figure 6—Dissolution of monoclinic or rhombic prismatic particles with shape ratios  $F_1 = 1/2$  and  $F_2 = 1/4$  (unbroken line, Eq. 25) and a hypothetical spherical particle (broken line) representing the approximation (Eq. 32) from which the equivalent spherical diameter is calculated (Eq. 33).

<sup>2</sup> The equation for a triclinic particle is not included because of its complexity and limited application, but it can be transformed to Eq. 25.



**Figure 7**—Graph of errors in the spherical approximation (Eq. 32) to the dissolution (Eq. 25) of a monoclinic or rhombic prismatic particle of different shape ratios. The error is weighted proportionally to the fraction undissolved ( $w/w_0$ ). Key: 1,  $F_2 = 1/6$ ; 2,  $F_2 = 1/4$ ; and 3,  $F_2 = 1/3$ ,  $F_1 = 1/2$ .

The basic assumption behind these derivations is that the rate of dissolution per unit surface area,  $J$ , remains constant during dissolution and is the same everywhere at the interface of the dissolving crystal. This assumption can only be approximately true in practice under complete sink conditions. The higher activity at the crystal edges results in a larger  $J$  value in these areas and, therefore, a "rounding off" of the shape, so that dissolution in the later stages is slower than that calculated. However, this should result in an im-

provement in the fit of the spherical approximation and sometimes may result in a closer fit to the real dissolution than the exact expressions given for isotropic conditions. Thus, the approximating curve (stippled line, Figs. 4 and 6) is above the calculated dissolution curve in the later stages. The true dissolution curve, because of the rounding off effect, is above the calculated curve and hence closer to the approximation.

Excellent agreement between experimental and calculated results was obtained for the dissolution of a multiparticulate system of particles, approximately tetragonal prismatic in shape, when the respective spherical approximations were applied (9).

#### REFERENCES

- (1) J. P. Cleave, *J. Pharm. Pharmacol.*, **17**, 698(1965).
- (2) J. Cobby, M. Mayersohn, and G. C. Walker, *J. Pharm. Sci.*, **63**, 725(1974).
- (3) I. C. Edmundson and K. A. Lees, *J. Pharm. Pharmacol.*, **17**, 193(1965).
- (4) R. J. Withey, *ibid.*, **23**, 573(1971).
- (5) A. W. Hixson and J. H. Crowell, *Ind. Eng. Chem.*, **23**, 923(1931).
- (6) P. Veng Pedersen and K. F. Brown, *J. Pharm. Sci.*, **64**, 1981(1975).
- (7) P. J. Niebergall, G. Milosovich, and J. E. Goyan, *ibid.*, **52**, 236(1963).
- (8) P. Veng Pedersen and K. F. Brown, *ibid.*, **64**, 1192(1975).
- (9) *ibid.*, **65**, 1442(1976).

#### ACKNOWLEDGMENTS AND ADDRESSES

Received May 2, 1975, from the Department of Pharmacy, University of Sydney, Sydney, N.S.W. 2006, Australia.

Accepted for publication December 10, 1975.

Supported in part by Grant 72.4244 from the National Health and Medical Research Council of Australia.

\* To whom inquiries should be directed.

## Experimental Evaluation of Three Single-Particle Dissolution Models

PETER VENG PEDERSEN\* and K. F. BROWN

**Abstract** □ The dissolution of the 60–85-mesh fraction of tolbutamide was investigated using a high precision, continuous recording, flow-through dissolution apparatus equipped with a dissolution cell; it was particularly suitable for kinetic analysis of multiparticulate systems. By using a time-scaling approach, experimental data are compared with theoretical calculations to evaluate, quantitatively, which of three single-particle dissolution models best describes the data and how well the multiparticulate kinetics can be explained mathematically. The nonspherical tolbutamide particles are replaced in the calculations by a hypothetical

system of spherical particles that appears to be log-normally distributed. This procedure permits the calculation of the intrinsic dissolution profile, considering both size distribution and particle shape effects.

**Keyphrases** □ Dissolution—tolbutamide, three single-particle models evaluated and compared, mathematical analysis □ Tolbutamide—dissolution, three single-particle models evaluated and compared, mathematical analysis

There are several kinetic models for single-particle dissolution. Experimental evaluation of these models has been based on multiparticulate dissolution data, but distribution and particle shape effects have not been considered. The general theory of multiparticulate dissolution was discussed previously (1). This theory was subsequently used to develop mathematical expressions for the dissolution of log-normally

distributed powders, considering three single-particle dissolution models (2).

A recent publication (3) dealt with the theory of single-particle dissolution in relation to particle shape. It gives directions for calculating the diameter of hypothetical spherical particles whose dissolution approximates nonspherical particles with minimum error. This paper demonstrates the application of